Available online at www.sciencedirect.com
ScienceDirect
Journal of Power Sources 162 (2006) 1357–1362
JOURNAL OF POWER SOURCES
www.elsevier.com/locate/jpowsour

Short communication

Preparation and electrochemical studies of Fe-doped $Li_3V_2(PO_4)_3$ cathode materials for lithium-ion batteries

Manman Ren, Zhen Zhou *, Yuzhan Li, X.P. Gao, Jie Yan

Institute of New Energy Material Chemistry, Department of Materials Chemistry, Nankai University, Tianjin 300071, China

Received 5 May 2006; received in revised form 21 June 2006; accepted 12 August 2006
Available online 15 September 2006

Abstract

The Fe-doped $Li_3V_2(PO_4)_3$ cathode materials for Li-ion batteries were synthesized by a conventional solid-state reaction, and the Fe-doping effects on the Li electrochemical extraction/insertion performance of $Li_3V_2(PO_4)_3$ were investigated by galvanostatic charge/discharge and cyclic voltammetry measurements. The optimal Fe-doping content x is 0.02–0.04 in $Li_3Fe_xV_{2-x}(PO_4)_3$ system. The Fe-doped $Li_3V_2(PO_4)_3$ samples showed a better cyclic ability between 3.0 and 4.9 V, for example, the discharge capacity of $Li_3Fe_{0.02}V_{1.98}(PO_4)_3$ was 177 mAh g^{-1} in the 1st cycle and 126 mAh g^{-1} in the 80th cycle. The retention rate of discharge capacity is about 71%, much higher than 58% of the undoped system. The improved electrochemical performances of the $Li_3V_2(PO_4)_3$ could be attributed to the increased electrical conductivity and structural stability deriving from the incorporation of the Fe^{3+} ions.

Keywords: Li-ion batteries; Cathode materials; Cyclic voltammetry (CV); $Li_3V_2(PO_4)_3$; Fe-doping

1. Introduction

Rechargeable lithium-ion batteries are considered as one of the most advanced energy storage systems; however, the development of Li-ion batteries cannot keep up with the fast development of the current information-rich mobile society, so more efforts have been made to explore novel Li insertion materials for both cathodes and anodes [1–4]. In commercial Li-ion cells cobalt-based oxide is utilized as the cathode material [5], but its high cost prohibits the large-scale use. Recently, considerable studies have been performed to lithium conducting phosphates such as $LiFePO_4$, $LiMnPO_4$ and $Li_3V_2(PO_4)_3$ [6–21]. These materials contain both mobile Li cations and redox-active metals within a rigid phosphate network, and display remarkable electrochemical and thermal stability as well as comparable energy density [17]. Among the above phosphates, monoclinic lithium vanadium phosphate, α-$Li_3V_2(PO4)_3$, is a highly promising cathode material proposed for Li-ion batteries. The monoclinic $Li_3V_2(PO_4)_3$ with three-dimensional (3D) framework contains three independent lithium sites. The large poly-anion instead of the smaller O^{2-} ions in an open 3D framework helps to stabilize the structure and allows fast ion migration [10,11]. It was believed that in $Li_3V_2(PO_4)_3$ only two Li^+ ions could be cycled reversibly; however, it has been demonstrated recently that all the three Li^+ ions can be exacted at room temperature on oxidation [10,11,13] and then high capacity can be expected in this system.

In the $Li_3V_2(PO_4)_3$ system, vanadium can also be substituted completely with some other metals such as Ti, Fe, Cr, Al and Ni [13,19,22] to form new $Li_3M_2(PO_4)_3$ systems. However, the part substitution of V with other metals is also worth exploring, since the doping of lithium transition metal oxides has proved effective to improve their Li extraction/insertion performance and increase their electronic conductivity. In this paper, the Fe-doping effects were investigated on the electrochemical Li extraction/insertion properties of $Li_3V_2(PO_4)_3$, and it showed that doping with small amount of Fe resulted in improvement of discharge capacity and cycling stability in the $Li_3V_2(PO_4)_3$ system.

* Corresponding author. Tel.: +86 22 23498941; fax: +86 22 23498941.
E-mail address: zhouzhen@nankai.edu.cn (Z. Zhou).

0378-7753/$ – see front matter © 2006 Published by Elsevier B.V.
doi:10.1016/j.jpowsour.2006.08.008

2. Experimental

2.1. Preparation of $Li_3Fe_xV_{2-x}(PO_4)_3$ ($0.00 \le x \le 0.06$)

The $Li_3Fe_xV_{2-x}(PO_4)_3$ samples, where $x = 0.01$, 0.02, 0.04 and 0.06, were synthesized by a solid-state reaction from a mixture of stoichiometric Li_2CO_3, V_2O_5, $NH_4H_2PO_4$, Fe_2O_3 and carbon with high surface area. The carbon was 1 wt% excess over the stoichiometric amount. The mixture was initially heated to 300 °C in an argon atmosphere for 4 h to decompose Li_2CO_3 and $NH_4H_2PO_4$. The product was then ground, pressed into pellets and then heated to 900 °C with a stream of pure argon gas for 8 h. Subsequently, the same procedure was repeated for the above product to ensure the thorough completion of the solid-state reaction. The undoped $Li_3V_2(PO_4)_3$ sample was also prepared for comparison through the same method except the addition of Fe_2O_3.

2.2. Sample characterization

Structural and crystallographic analyses of the products were taken from the X-ray diffraction (XRD) using the D/MAXIII diffractometer with Cu Kα radiation. The X-ray photoelectron spectroscopy (XPS) was obtained for the $Li_3Fe_{0.02}V_{1.98}(PO_4)_3$ sample by using Kratos Axis Ultra DLD spectrometer with monochromatic Al Kα radiation ($h\nu = 1486.6$ eV). The samples were also observed using the Hitachi S-3500N scanning electron microscopy (SEM).

2.3. Electrical conductivity measurements

The $Li_3Fe_{0.02}V_{1.98}(PO_4)_3$ and undoped $Li_3V_2(PO_4)_3$ powders were consolidated into the disk-shaped specimens with 1.45 cm in diameter and ~1.3 mm in thickness by the uniaxial pressing at 15 MPa in a mold. The electrical conductivities of the $Li_3Fe_{0.02}V_{1.98}(PO_4)_3$ and undoped $Li_3V_2(PO_4)_3$ samples were measured by a direct Volt–Ampere method.

2.4. Electrochemical tests

Electrochemical performances of the samples were evaluated in Li test cells. The cathode material was prepared by mixing the products with acetylene black and polytetrafluoroethylene (PTFE) with a weight ratio of 85:10:5 in ethanol to ensure the homogeneity. After the ethanol was evaporated, the mixture was rolled into a sheet, and cut into circular strips of 8 mm in diameter. The strips were then dried at 100 °C for 10 h. Lithium metal was used as an anode. The electrolyte was composed of a 1 M $LiPF_6$ dissolved in ethylene carbonate/dimethyl carbonate with the weight ratio of 1:1. The three parts were assembled into test cells in an argon-filled dry glove box, and then the cells were measured using a Land CT2001 battery tester. The electrochemical measurements were performed at a *C*/5 rate in a voltage range of 3.0–4.9 V at room temperature, and the cells were also tested at a *C*/2 rate as well as at a higher temperature (55 °C).

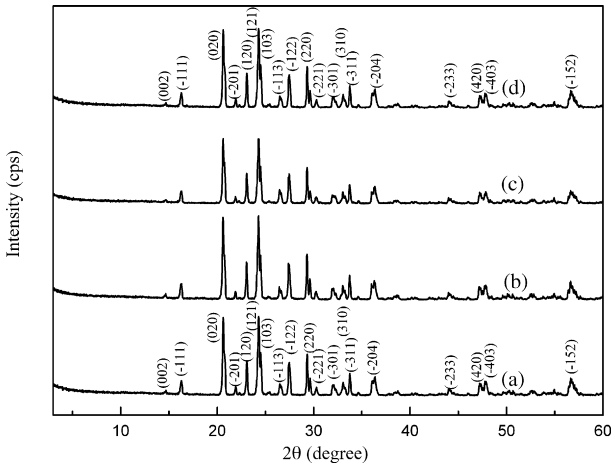

Fig. 1. Typical XRD patterns for $Li_3Fe_xV_{2-x}(PO_4)_3$ (a) $x = 0$, (b) $x = 0.02$, (c) $x = 0.04$ and (d) $x = 0.06$.

2.5. Cyclic voltammetric measurements

The cyclic voltammetric (CV) measurements were carried out with a CHI 600A electrochemical analyzer. The CV curves for the above test cells were recorded in the potential range of 3.0–4.9 V at a scan rate of 0.05 mV s^{-1} at room temperature.

3. Results and discussion

3.1. Sample characterization

The XRD patterns of the Fe-doped and undoped $Li_3V_2(PO_4)_3$ samples are shown in Fig. 1. The Fe-doped samples with various Fe contents all show a monoclinic $Li_3V_2(PO_4)_3$ phase, similar to the undoped sample. Table 1 shows the cell parameters of $Li_3V_2(PO_4)_3$ and $Li_3Fe_{0.02}V_{1.98}(PO_4)_3$, and it can be seen that the cell parameters of $Li_3V_2(PO_4)_3$ decreased after Fe-doping. The oxidation states of V and Fe dopant were studied by XPS, and Fig. 2 shows the Fe_{2p} and V_{2p} XPS core levels for the $Li_3Fe_{0.02}V_{1.98}(PO_4)_3$ sample. The V_{2p} core level fits to a single peak with a binding energy (BE) of 517.2 eV, matching well with that observed in V_2O_3 (517.3 eV) [23], so the oxidation state of V in $Li_3Fe_{0.02}V_{1.98}(PO_4)_3$ was +3. The Fe_{2p} XPS also shows a single peak with a BE of 711.8 eV, similar to that observed in Fe_2O_3 (711.7 eV) [14], so the oxidation state of Fe in $Li_3Fe_{0.02}V_{1.98}(PO_4)_3$ was also +3.

The SEM image of the $Li_3Fe_{0.02}V_{1.98}(PO_4)_3$ powder is shown in Fig. 3. The Fe-doped $Li_3V_2(PO_4)_3$ particles congregated together with an average size of 4 μm.

Table 1
Cell parameters of $Li_3V_2(PO_4)_3$ and $Li_3Fe_{0.02}V_{1.98}(PO_4)_3$

	a (Å)	*b* (Å)	*c* (Å)	*β* (°)	*V* (Å^3)
$Li_3V_2(PO_4)_3$	8.606	8.591	12.036	90.61	899.8
$Li_3Fe_{0.02}V_{1.98}(PO_4)_3$	8.596	8.592	11.998	90.38	886.1

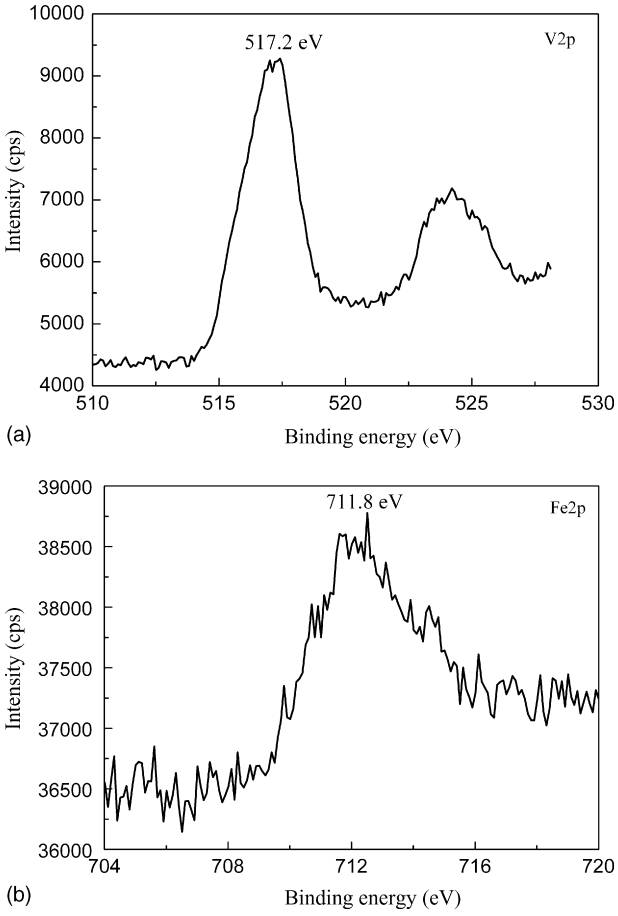

Fig. 2. XPS core level of V_{2p} and Fe_{2p} from $Li_3Fe_{0.02}V_{1.98}(PO_4)_3$.

3.2. Galvanostatic electrochemical measurements

The initial charge/discharge curves are shown in Fig. 4 for the $Li/Li_3Fe_{0.02}V_{1.98}(PO_4)_3$ and $Li/Li_3V_2(PO_4)_3$ test cells at *C*/5 charge/discharge rate in the range of 3.0–4.9 V at room temperature. It can be seen that four plateaus appear in the charge process and two plateaus in the discharge process, which is the characteristic of the electrochemical reactions between two phases. The charge curves of the two samples are almost the same, but the discharge plateau is a little longer in the discharge curve of the Fe-doped $Li_3V_2(PO_4)_3$. From the initial discharge capacity, the doping effects of Fe are not so apparent, but the significant effects can be observed from the long-term charge/discharge cyclic performances in the following tests.

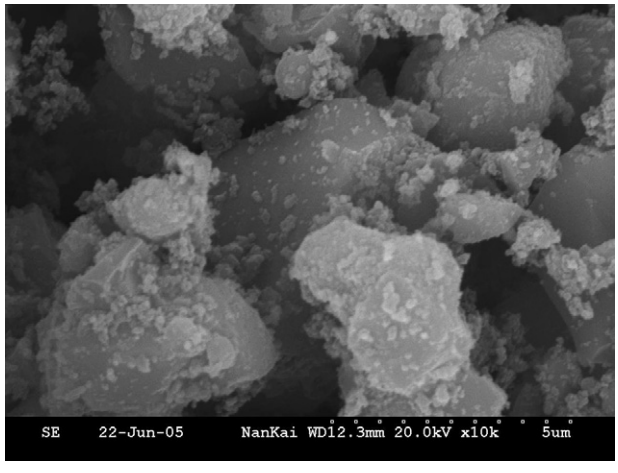

Fig. 3. SEM image of $Li_3Fe_{0.02}V_{1.98}(PO_4)_3$ sample.

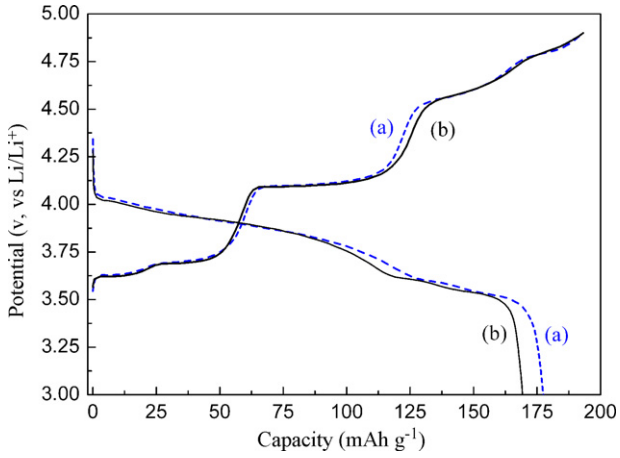

Fig. 4. Typical charge/discharge curves of Fe-doped (a) and undoped $Li_3V_2(PO_4)_3$ (b).

The results of charge/discharge cycles at *C*/5 rate in the range of 3.0–4.9 V at room temperature are shown in Fig. 5 for the undoped and the Fe-doped $Li_3V_2(PO_4)_3$ samples with various Fe contents. All the Fe-doped $Li_3V_2(PO_4)_3$ samples exhibit higher discharge capacity after about 50 cycles than the undoped samples, meaning that the Fe-doped $Li_3V_2(PO_4)_3$ samples had better cyclic ability and electrochemical stability. Though the initial discharge capacity of the undoped $Li_3V_2(PO_4)_3$ was rather large, the discharge capacity decreased more sharply than that of the Fe-doped $Li_3V_2(PO_4)_3$ samples. Namely, in the undoped $Li_3V_2(PO_4)_3$ system, the discharge capacities for the 1st and 80th cycle were 169 and 98.6 mAh g^{-1}, respectively,

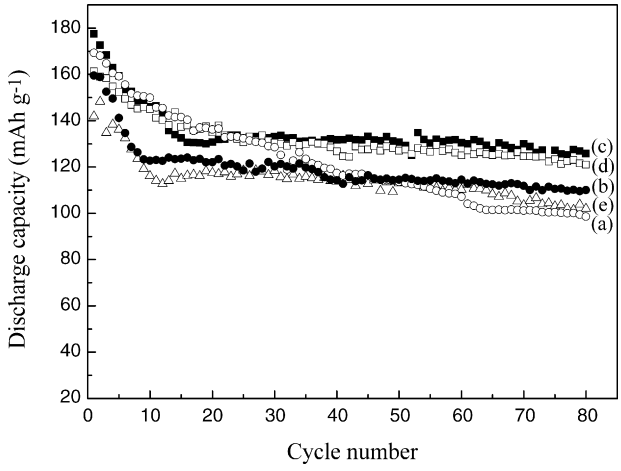

Fig. 5. Discharge capacity as a function of cycle number at *C*/5 rate and 25 °C for various $Li_3Fe_xV_{2-x}(PO_4)_3$. (a) $x = 0.00$; (b) $x = 0.01$, (c) $x = 0.02$, (d) $x = 0.04$ and (e) $x = 0.06$.

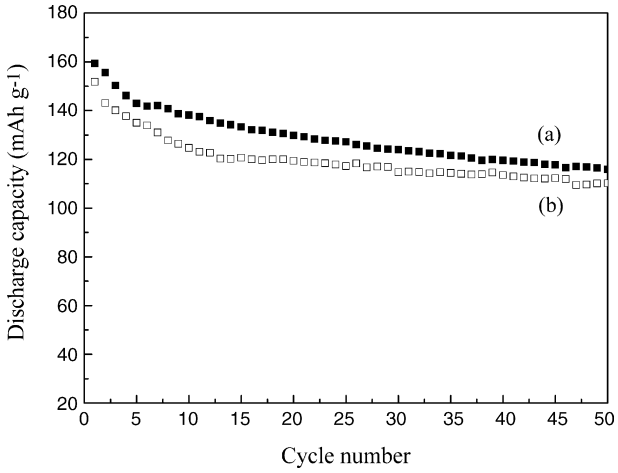

Fig. 6. Cyclic lifetime at $C/2$ rate of $Li_3Fe_{0.02}V_{1.98}(PO_4)_3$ at 55 °C (a) and 25 °C (b).

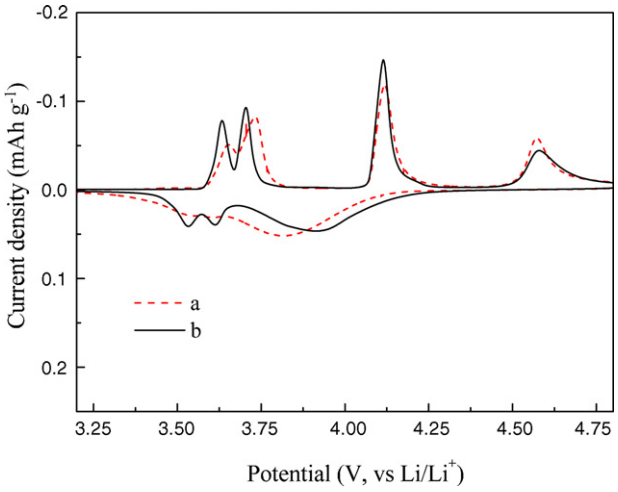

Fig. 7. CV curves of $Li_3V_2(PO_4)_3$: (a) and $Li_3Fe_{0.02}V_{1.98}(PO_4)_3$ (b).

so the discharge capacity retention was only 58%. However, in the case of the $Li_3Fe_xV_{2-x}(PO_4)_3$ samples, when $x = 0.02$ or 0.04, the discharge capacities decreased quickly only during the first 20 cycles, but then kept quite constant during the following cycles, e.g., the capacities of the 1st and 80th cycles for $Li_3Fe_{0.02}V_{1.98}(PO_4)_3$ were 177 and 126 mAh g^{-1}, respectively, with the discharge capacity retention of 71%. The result displays that doping with small amount of Fe resulted in better cycling stability. Both low Fe content such as $x = 0.01$ and too high Fe content such as $x = 0.06$ did not effectively restrain the capacity degradation of the $Li_3V_2(PO_4)_3$ cathode material during cycles. It is easy to understand that too small amount of Fe dopant only gives slight effect on the $Li_3V_2(PO_4)_3$ crystal structure, but the existence of too many Fe ions in the crystal lattice may induce large changes to the structure and cause the phase instability. Therefore, the optimal Fe-doping content x was 0.02–0.04 in this investigation, and the $Li_3Fe_{0.02}V_{1.98}(PO_4)_3$ sample will be taken as an example in the following measurements.

The charge/discharge cyclic tests were also performed at $C/2$ rate as well as at a higher temperature (55 °C), and are shown in Fig. 6, compared with the corresponding results at room temperature. At higher temperature the $Li_3Fe_{0.02}V_{1.98}(PO_4)_3$ sample exhibited a greater discharge capacity and better cycle ability, which may be attributed to the higher Li diffusion rate in the interstitial space of $Li_3V_{1.98}Fe_{0.02}(PO_4)_3$ at elevated temperatures [14,23].

3.3. CV measurements

The CV curves were recorded for the $Li_3V_2(PO_4)_3$ and $Li_3Fe_{0.02}V_{1.98}(PO_4)_3$ system and are shown in Fig. 7. There are four oxidation peaks and three reduction peaks in the CV curves for the $Li_3Fe_{0.02}V_{1.98}(PO_4)_3$ system. The four oxidation peaks are located around 3.6, 3.7, 4.1 and 4.6 V, respectively, and three reduction peaks are located around 3.5, 3.6 and 3.9 V, respectively, indicating the phase transition occurring during Li extraction and insertion, in good agreement with the charge/discharge curves shown in Fig. 5. The oxidation peaks located around 3.6 and 3.7 V correspond to the removal of the first Li in two steps, because there is an ordered $Li_{2.5}V_2(PO_4)_3$ phase [10]. However, the second Li is extracted through one single step around 4.1 V. The first two Li ions extraction is also associated with the V^{3+}/V^{4+} redox couple. The reaction occurring around 4.6 V is the extraction of the third lithium, associated with the V^{4+}/V^{5+} redox couple. The above results are in good agreement with those reported by Saidi et al. [10]. During the anodic process, the three peaks located around 3.5, 3.6 and 3.9 V can be attributed to the re-insertion of the three Li ions, associate with the V^{5+}/V^{4+} and V^{4+}/V^{3+} redox couples.

In the Fe-doped system, the shape of the CV curve does not change greatly, indicating that the Fe-doping did not change the $Li_3V_2(PO_4)_3$ structure and the regime for the phase transition and redox couple during the electrochemical Li extraction/insertion process. However, there are some apparent differences that can be observed in the CV curve of the doped system. Firstly, the anodic peaks at 3.5 and 3.6 V are separated apparently in the Fe-doped $Li_3V_{1.98}Fe_{0.02}(PO_4)_3$ system. Secondly, the anodic peaks all shift to the higher potentials, and then the potential differences between anodic peaks and cathodic peaks become smaller, showing the enhancement of electrode reaction reversibility.

3.4. XRD patterns after long-term cycles

The XRD patterns of the $Li_3Fe_{0.02}V_{1.98}(PO_4)_3$ (a) and $Li_3V_2(PO_4)_3$ (b) sample after 80 charge/discharge cycles are presented in Fig. 8. Fig. 8 shows a similar XRD pattern to that of the original $Li_3Fe_{0.02}V_{1.98}(PO_4)_3$ phase in Fig. 1(a). This result indicates that the original monoclinic $Li_3Fe_{0.02}V_{1.98}(PO_4)_3$ phase could be recovered even after many charge/discharge cycles, and only the XRD peaks became wider, which is the usual phenomena resulting from the pulverization of active materials during long-term cycles [24].

3.5. Electronic conductivity measurements

The electrical conductivity of $Li_3V_2(PO_4)_3$ was measured as 0.096 S cm^{-1}, but the $Li_3Fe_{0.02}V_{1.98}(PO_4)_3$ sample showed a

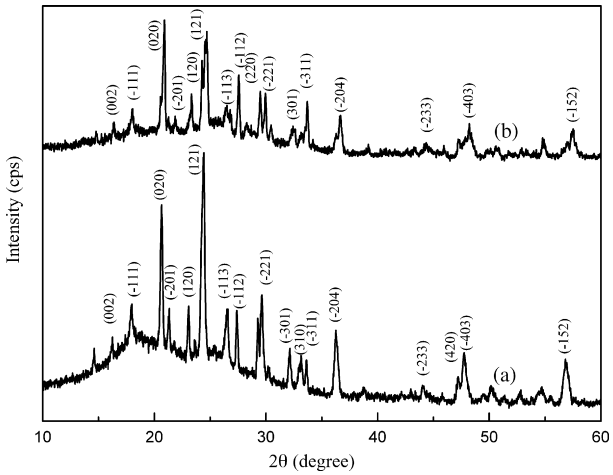

Fig. 8. XRD pattern of (a) $Li_3Fe_{0.02}V_{1.98}(PO_4)_3$ and (b) $Li_3V_2(PO_4)_3$ after 80 charge/discharge cycles.

more than one order of magnitude higher electrical conductivity, 1.6 S cm^{-1}. The electrical conductivity of $Li_3V_2(PO_4)_3$ was apparently increased due to the Fe-doping, which is preferable for the enhancement in electrochemical Li insertion performances of phosphate-based Li intercalation materials.

It has been found from calculations that transition metals do not interact much when mixed in the NASICON-like compounds, so $Li_3(M_xN_{2-x})(PO_4)_3$ will show the features of the M and N redox couples separately. Given the large physical distance between the metal sites and the large "electronic separation" induced by the phosphate groups, it is natural that the alloying effect on the redox couple is very weak [14]. It was also observed in our investigation that the Fe-doping does not change the regime for electrochemical Li extraction/insertion process in the $Li_3V_2(PO_4)_3$ system. However, the volume of $Li_3Fe_2(PO_4)_3$ is a little smaller than that of $Li_3V_2(PO_4)_3$ in the monoclinic phase (Table 1), and also the V^{4+}/V^{5+} redox couple is active, but the Fe^{4+}/Fe^{5+} redox couple is inactive [14]. It can be seen from Fig. 8 that sharper peaks appear in the XRD patterns of $Li_3Fe_{0.02}V_{1.98}(PO_4)_3$, indicating that $Li_3V_2(PO_4)_3$ phase was well kept after long-term charge/discharge cycles. Therefore, it is possible that the existence of Fe ions might counteract the volume shrinking/swelling during the Li^+ reversible extraction/insertion, and then increase the stability of $Li_3V_2(PO_4)_3$ phase in the charge/discharge cycles. It has been reported that the phase stability of orthorhombic $Li_3V_2(PO_4)_3$ was enhanced by Zr-doping [25]. On the other hand, the existence of Fe will cause some local defects in the crystal structure, leading to the increase of electrical conductivity and ionic diffusion, so the cyclic performances of the $Li_3V_2(PO_4)_3$ system were apparently improved through the doping of small amount of Fe. Further investigations are still necessary to completely clarify the Fe-doping effects in the $Li_3V_2(PO_4)_3$ system.

4. Conclusion

The undoped and Fe-doped $Li_3V_2(PO_4)_3$ cathode materials were synthesized by conventional solid-state reactions. X-ray diffraction results show that a monoclinic phase was obtained, and V and Fe are both +3 in valence according to XPS analysis. The Fe-doped $Li_3V_2(PO_4)_3$ cathode materials show better charge/discharge cyclic stability. The discharge capacity of $Li_3Fe_{0.02}V_{1.98}(PO_4)_3$ was 177 mAh g^{-1} in the 1st cycle, and 126 mAh g^{-1} in the 80th cycle, with the 71% retention rate of discharge capacity, much higher than 58% of the undoped system. The optimal Fe-doping content x is 0.02–0.04 in $Li_3Fe_xV_{2-x}(PO_4)_3$ to achieve high discharge capacity and good cyclic stability. According to the CV measurements, the electrode reaction reversibility is enhanced due to the Fe-doping. The Fe-doping proposed in this investigation may improve the electrochemical performances and cyclic stability of $Li_3V_2(PO_4)_3$ cathode materials for Li-ion batteries.

Acknowledgements

This work was supported by the 973 Program (2002CB211800) and NCET (040219) of China and the authors thank that Tianjin Lishen Battery Co., Ltd. supplied some of the materials used in the assemble of Li ion test cells.

References

[1] J.M. Tarascon, M. Armand, Nature 414 (2001) 359.
[2] M. Winter, J.O. Besenhard, M.E. Spahr, P. Novak, Adv. Mater. 10 (1998) 725.
[3] Z. Zhou, J.J. Zhao, X.P. Gao, Z.F. Chen, J. Yan, P.V. Schleyer, M. Morinaga, Chem. Mater. 17 (2005) 992.
[4] W.H. Pu, X.M. He, J.G. Ren, C.R. Wan, C.Y. Jiang, Electrochim. Acta 50 (2005) 4140.
[5] T. Kerr, J. Gaubicher, L.F. Nazar, Electrochem. Solid-State Lett. 3 (2000) 460.
[6] A. Yamada, S.C. Chung, J. Electrochem. Soc. 148 (2001) A960.
[7] A. Yamada, M. Hosoya, S.C. Chung, Y. Kudo, K. Hinokuma, K.-Y. Liu, Y. Nishi, J. Power Sources 119–121 (2003) 232.
[8] S. Okada, S. Sawa, M. Egashira, J. Yamaki, M. Tabuchi, H. Kageyama, T. Konishi, A. Yoshino, J. Power Sources 97–98 (2001) 430–432.
[9] S.Y. Chung, J.T. Bloking, Y.M. Chiang, Nat. Mater. 1 (2002) 123.
[10] M.Y. Saidi, J. Barker, H. Huang, J.L. Sowyer, G. Adamson, J. Power Sources 119–112 (2003) 266.
[11] M.Y. Saidi, J. Barker, H. Huang, J.L. Swoyer, G. Adamson, Electrochem. Solid State Lett. 12 (2002) A149.
[12] S.C. Yin, H. Grond, P. Strobel, H. Huang, L.F. Nazar, J. Am. Chem. Soc. 125 (2003) 326.
[13] H. Huang, S.C. Yin, T. Kerr, N. Taylor, L.F. Nazar, Adv. Mater. 14 (2002) 1525.
[14] D. Morgan, G. Ceder, M.Y. Saidi, J. Barker, J. Swoyer, H. Huang, G. Adamson, Chem. Mater. 14 (2002) 4684.
[15] S. Patoux, C. Wurm, M. Morcrette, G. Rousse, C. Masquelier, J. Power Sources 119–121 (2003) 278.
[16] S.C. Yin, P.S. Strobel, H. Grondey, L.F. Nazar, Chem. Mater. 16 (2004) 1456.
[17] S.C. Yin, H. Grondey, P. Strobel, M. Anne, L.F. Nazar, J. Am. Chem. Soc. 125 (2003) 10402.
[18] M. Sato, S. Tajimi, H. Okawa, K. Uematsu, K. Toda, Solid State Ionics 152–153 (2002) 247.
[19] J. Barker, M.Y. Saidi, US Patent 5,871,866 (1999).
[20] J. Barker, M.Y. Saidi, J.L. Swoyer, J. Electrochem. Soc. 150 (2003) A684.
[21] M. Higuchi, H. Katayama, Y. Azuma, M. Yukawa, M. Suhara, J. Power Sources 119–121 (2003) 258.

[22] A.S. Andersson, B. Kalska, P. Eyob, D. Aernout, L. Häggström, J.O. Thomas, Solid State Ionics 140 (2001) 63.
[23] A. Van der Ven, G. Ceder, Meeting Abstract of Battery Division, Joint International Meeting, Honolulu, Hawaii, October 17–22, 1999 (Abstract no. 135).
[24] Z. Zhou, J. Yan, Y.X. Li, D.Y. Song, Y.S. Zhang, J. Power Sources 72 (1998) 236.
[25] M. Sato, H. Ohkawa, K. Yoshida, M. Saito, K. Uematsu, K. Toda, Solid State Ionics 135 (2000) 137.